Electrical Double Layers in Electrospray Propulsion

IEPC-2015-178／ISTS-2015-b-178

Presented at Joint Conference of 30th International Symposium on Space Technology and Science, 34th International Electric Propulsion Conference and 6th Nano-satellite Symposium
Hyogo-Kobe, Japan
July 4–10, 2015

Kento Masuyama* and Paulo C. Lozano†
Massachusetts Institute of Technology, Cambridge, MA 02139, USA

Ionic liquids, propellants in electrospray thrusters, cannot be described by classical dilute double layer theories; new theoretical frameworks have been introduced which predict multilayer double layer structures with different capacitance curves. These theories must be generalized to account for ion size asymmetry and be verified with experimental data. This work explores three different methods for measuring capacitance: cyclic voltammetry, impedance spectroscopy, and potentiostatic intermittent titration technique. All three methods gave qualitatively similar capacitance curves at moderate potentials, with a central hump and rising wings. Concentrated solution theories predict the wings to eventually decay, and this was seen in the impedance data as well as the positive wing in voltammetry.

Nomenclature

Z = complex impedance
k_B = Boltzmann constant
T = temperature
e = elementary charge
C = capacitance
ϵ_r = relative permittivity
ϵ_0 = vacuum permittivity
Q = charge
V = voltage
S = sweep rate
I = current
R = resistance
Y_o = constant phase element admittance
α = constant phase element parameter
t = time
a = ion diameter
λ_D = Debye length
l_c = electrostatic correlation length
c_0 = bulk concentration
N_A = Avogadro's number
ρ_m = mass density
$\bar{m}$ = molecular weight

*PhD Candidate, Department of Aeronautics and Astronautics, masuyama@mit.edu
†Associate Professor, Department of Aeronautics and Astronautics, plozano@mit.edu

I. Introduction

Electrospray propulsion systems present an opportunity to enable a wider scope of missions to pico- and nano-class satellites by providing attitude control, orbit walking, and other low-thrust maneuvers. Miniaturization of propulsion systems has proven difficult, with chemical and electric propulsion systems becoming disproportionately large compared to platforms such as the Cubesat. Ionic liquid ion source (ILIS) electrospray systems circumvent scaling issues by generating an ion beam from a liquid meniscus of order 1 µm and employing room temperature ionic liquid (RTIL) propellant whose negligible vapor pressure allows liquid-phase storage without pressurized tanks. RTILs are a class of solvent consisting purely of ions, for which careful selection of constituent cation and anion allows for tuning of physical parameters including conductivity, viscosity, and reduction or oxidation potentials. Ion beams are emitted when sufficient field strengths are achieved by applying a potential between the propellant and a downfield extractor electrode.[1] Either polarity ion can be emitted via electrospray,[2] thereby limiting spacecraft charging and obviating the need for separate cathodes as in traditional electric propulsion systems. These unique advantages have led to the development of a 15 µN thruster utilizing 480 distinct ion beams, 1 cm x 1 cm x 1 cm in size excluding the power processing unit but including propellant and propellant management.[3]

In order for electrospray propulsion to mature as a technology for widespread application, better understanding of emission physics is necessary. The RTIL menisci are supported on structures known as emitters, which can be capillaries,[4] externally wetted needles,[5] or porous tips;[6] emitters serve to transport propellant to the ion emission site and to amplify the applied electric field with its sharp geometry. Despite its importance, emitter design is based on ad-hoc methods. Selection of propellant RTILs is only slightly more rigorous with loose guidelines based on conductivity and ion sizes. After a working system is obtained, electrochemical reactions at the electrode in contact with the RTIL have been observed as life-limiting factors,[7,8] degrading both electrode geometry and RTIL composition. Emission and electrochemistry are both interfacial phenomena - to find better tools for propellant selection, thruster design, and operational parameters, it is necessary to probe the RTIL electrical double layer.

As RTILs have become popular for applications in energy storage, synthesis, and other fields, there is a growing body of work studying their electrochemical properties. However, the existing data have been measured in different systems under different conditions using different techniques, and observed trends are not always consistent. In this work, we measure the capacitance of the RTIL 1-ethyl-3-methylimidazolium tetrafluoroborate [emim][BF_4] using three different methods: electrochemical impedance spectroscopy (EIS), cyclic voltammetry (CV), and potentiostatic intermittent titration technique (PITT). An electrochemical cell was designed to work specifically with RTILs, particularly to operate under vacuum for maintaining purity. Using the same system and the same preparation, we are able to better compare data across different measurement techniques. We conclude with a discussion of trends in the capacitance measurements, which deviate from classical double layer theory due to high ion concentration. A framework is proposed for analyzing double layer charging in thruster electrodes simulating operating conditions.

II. Experimental Setup

II.A. Ionic Liquid Preparation

The [emim][BF_4] ionic liquid was obtained from Iolitec Inc. at $> 98\%$ purity. As with many RTILs it is hydrophilic, absorbing ambient moisture within minutes if left open. The RTIL was stored in a nitrogen-purged dry box, and immediately preceding each experiment, the RTIL was introduced into the electrochemical cell and held under vacuum for 10 hours to remove residual water. Particular care is necessary at the beginning of pumping down, as water vapor bubbles can coalesce into large bubbles, whose bursting can displace significant quantities of RTIL from the working area.

II.B. Electrochemical Cell

A parallel plate electrochemical cell was designed specifically for use with RTILs, shown in Fig. 1. The working and counter electrodes (WE and CE, respectively) are identical, machined from 316 stainless steel ANSI 10-34 bolts. Stainless steel is resistant to corrosion and degradation, and also has good machineability which was necessary for producing a flat working area of known area. The end of the bolt is turned down to a diameter of 1.5 mm and faced on a lathe. The face is progressively smoothed with 500, 1500, and 2500 grit

sandpaper, with a sonic bath cleaning in between each. It is further polished on a 0.1 µm Buehler polishing pad, and finished with a 20 nm fused silica suspension to give a mirror-like surface. After cleaning with acetone and isopropanol, the bolts are given a final sonic bath in deionized water. The bolts are then back-sputtered and coated with ≈ 50 nm of platinum with a 15 nm titanium adhesion layer via sputter deposition. As platinum does not readily react, it makes for a good electrode surface but does not bond well to the steel surface; the titanium layer helps to maintain a better bond and is often used for platinum coating, including sputtering and electroplating. The side surfaces of the turned down section is coated with a thin layer of non-conducting epoxy to isolate the working area of the electrode.

The cell casing is machined from PEEK, a hard plastic with good outgassing properties for use in vacuum environments. The WE and CE are screwed in from either side, so that the separation distance is adjustable by turning the bolt. In order to hold the RTIL in place, a FEP tube is attached to the end of the WE. A small hole in the FEP tubing, near the plane of the WE surface, is used to insert a 0.01 in. 99.99% pure platinum wire to serve as the quasi-reference (QRE). The QRE is placed as close to the WE as possible to reduce electrolyte resistance and sealed in place to prevent leakage.

For each experiment, ≈ 5 µL of RTIL is introduced into the FEP tube. After an initial drying under rough vacuum, the CE is moved into position with the separation distance checked under a microscope. The cell is then placed back in the vacuum chamber for its 10 hour drying.

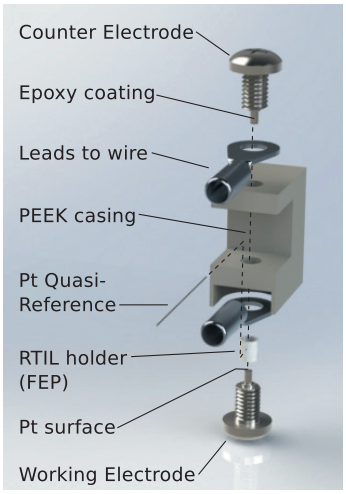

Figure 1. Exploded view of electrochemical cell for use in vacuum. WE and CE Pt surfaces areas are isolated by epoxy. QRE is Pt wire.

II.C. Experimental Methods

Electrochemical tests were conducted on two devices: Gamry Reference 3000 and Princeton Applied Research VersaSTAT 3. All tests were conducted three or more times to verify repeatability and gave similar results. Previous research showed that voltage scans must start at open circuit potential (OCV) to give reproducible results,[9] so all experiments started were preceeded by 1 h of monitoring the open circuit potential and any bias voltages started from that reference point. At the beginning of experiments the OCV was small as expected from using the same material electrodes, on the order of 10 mV.

Voltammetry is often used to find the electrochemical window, defined as the range between the oxidation and reduction potentials within which no significant Faradaic reactions occur. The current stays close to zero within the window, rising sharply at the limits upon the onset of reactions. Although close to zero, the current is not exactly zero—there is a small current associated with charging of the double layer at the electrode—electrolyte interface. Assuming no reactions, the double layer acts as a capacitor storing charge. In order to probe this capacitance, we ran CV well within the electrochemical window. CV applies a voltage ramp at constant sweep rate, selected as S =1, 5, 10, and 50 mV s^{-1}, starting from OCV to the upper limit ≈ 1.2 V and immediately reversing direction to the lower limit ≈ −1 V, before finally returning to the OCV.

Impedance spectroscopy applies a small AC voltage perturbation about a DC bias potential. By measuring the magnitude and phase shift of the response current, the complex impedance Z is found. This can then be fit with equivalent circuit models to obtain parameters such as resistance and capacitance. We scanned the same potential range ± 1.2 V in 50 mV intervals in order to obtain the variation of capacitance with applied potential. Each bias potential was tested with AC perturbations at frequencies ranging from 0.1 Hz to 1 MHz.

PITT is a sequence of small voltage steps (smaller than thermal voltage $\frac{k_B T}{e}$, where k_B is Boltzmann constant, T is temperature, and e is elementary charge), in which the resulting transient currents are analyzed. It is a common technique for probing the diffusivities of reactants in electrochemical systems; however within the electrochemical window, we can again use this technique to probe the charging current of the double layer. Starting from OCV, we apply 10 mV steps, each held for 5 s. We can then fit a model for RC current decay to obtain capacitance as a function of bias potential.

III. Results

An ideal linear capacitor has constant capacitance C per area A defined by permittivity $\epsilon_r\epsilon_0$ and separation distance d,

$$C = \frac{Q}{V} = \frac{\epsilon_r\epsilon_0}{d}A \tag{1}$$

where Q and V are the charge and voltage stored in the capacitor. Rearranging and differentiating with respect to time

$$\frac{d}{dt}CV = C\frac{dV}{dt} = CS = \frac{dQ}{dt} = I \tag{2}$$

suggests that for constant C and S, a constant current I is the response.

Figure 2 shows the actual response of the [emim][BF_4] double layer capacitor. Although the current magnitude is not constant, scaling by the sweep rate gives very consistent results. Note that the dimensions are consistent with capacitance, specifically $\mathrm{nA\,s\,mV^{-1}} = \mu\mathrm{F}$. This indicates that despite the nonlinear response, the observed current can in fact be interpreted as double layer capacitor charging. The different potential regions covered by the positive sweep (blue) and negative sweep (red, scaled by $-S$) is due to the nonlinear response; in the ideal case treated mathematically above, the current would instantly jump from its positive value to a negative value. However in real systems, there is a lag over which the current decreases over a finite time, and this region has been omitted for clarity. The potential of zero charge (PZC) is often used as a reference point, where the double layer has zero net charge. Depending on the selection of electrode materials, the PZC is not necessarily at OCV. When a potential positive of PZC is applied, the anion is attracted into the double layer and is the primary driver of the capacitance. At negative potentials, the cation becomes the counterion primarily drawn into the double layer. From Eq. 1 we see that the capacitance varies with some length scale; this is, as discussed below, in turn dependent on the counterion size. While many concentrated electrolyte theories assume symmetric ion sizes (leading to symmetric capacitance curves), we see that many RTILs have large asymmetries in cation and anion size. This is expected to cause different values of capacitance above and below PZC.

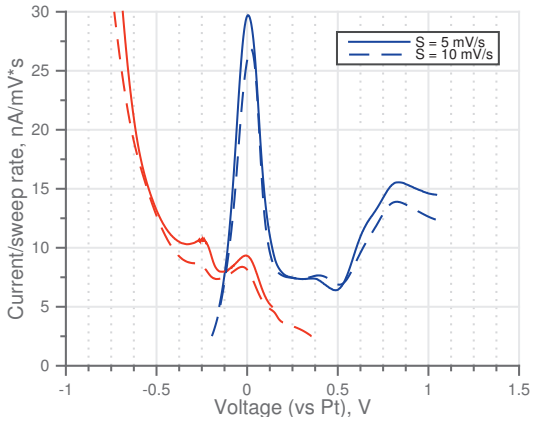

Figure 2. Cyclic voltammetry current response scaled by sweep rate. Blue line for positive sweep, Red line for negative sweep.

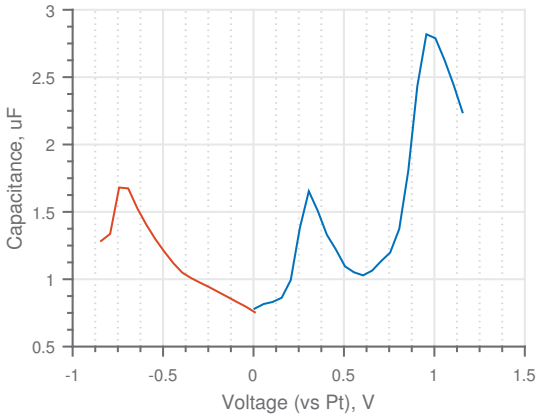

Figure 3. Capacitance at f =0.1 Hz at various DC bias potentials, calculated from fitting impedance data with a series resistor+CPE equivalent circuit.

In order to interpret impedance data, it is necessary to assume an equivalent circuit model for the experimental interface. Within the electrochemical window we assume no Faradaic reactions, i.e., ideally polarizing electrodes. In this case, we can assign a simple equivalent circuit of a resistance in series with a capacitor. With real systems, as was seen in the voltammetry results, capacitors do not behave ideally; as such, we make use of a constant phase element (CPE) which accounts for imperfect capacitor behavior. The impedance of this circuit can be calculated as

$$Z = R + \frac{1}{Y_o(\omega i)^\alpha} \tag{3}$$

where R is resistance, Y_o is CPE admittance, ω is frequency, and α is the correction parameter indicating deviation from ideal capacitor behavior. Using this model, we can calculate capacitance from the data and the fitted parameters as

$$C = -(\omega Z_{imag})^{-1} = \frac{Y_o\omega^{\alpha-1}}{\sin\frac{\pi}{2}\alpha} \tag{4}$$

For our data shown in Fig. 3, the full frequency spectrum was tested at each bias potential and fitted with Eq. 3. In practice, the magnitude and phase of the complex impedance Z were fitted on a Bode plot. One representative fit gave the values $[R, Y_o, \alpha] = [29.18, 1.02 * 10^{-7}, 0.90]$, with χ^2 =0.98 and 0.93 for the magnitude and phase fits, respectively. This indicates that the assigned equivalent circuit is a good model of the actual behavior. As can be seen from the CPE component of the impedance in Eq. 3 and in Eq. 4, the capacitance is frequency-dependent. The capacitance decreases with frequency, and so the smallest measured frequency of 0.1 Hz was selected for the presented data; capacitances at other frequencies showed the same trends shifted to smaller magnitudes. The peaks at ≈-0.7 and 1.0 V agree qualitatively with previously reported data for other RTILs,[10] however the peak in the middle is not a feature found in their data. Also note that the distance between the peaks correspond well to those seen in the voltammetry results, although the magnitudes differ by an order of magnitude. Slight shifts in potential may be explained by drift of the QRE, a problem inherent with use of references that are not in true thermal equilibrium with the electrolyte.

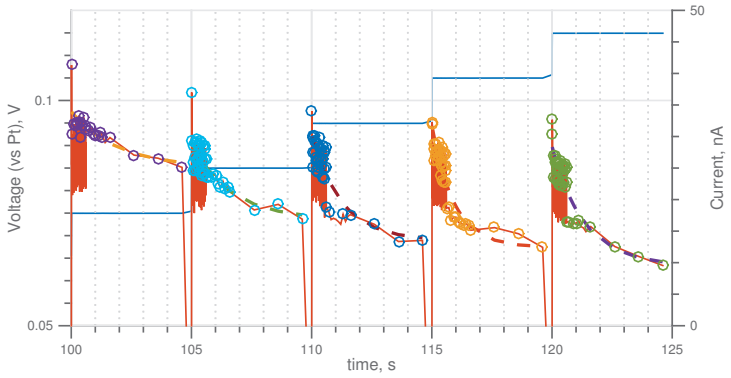

Figure 4. Voltage steps and current response during PITT experiment. Solid line shows raw data, circles indicate filtered data used for fitting, and dotted line is the exponential fit.

PITT is a common technique in analyzing batteries; however, we could not find any references that have tried applying this to RTIL double layer charging studies. As small voltage steps are applied, there is an initial spike in current of order $I_0 \sim \frac{V_{step}}{R}$. This current decays as the double layer charges to equilibrate with the applied potential. Again assuming the system to be modeled by a resistor in series with a capacitor, we hypothesized that this gives a pure RC decay response. This was confirmed by the results shown in Fig. 4. By fitting each exponential decay with the equation

$$I = I_0 e^{-(t-t_0)/RC} + \text{const.} \tag{5}$$

we are able to obtain capacitance values at each voltage step, as shown in Fig. 5.

Note again the similarity of the curve to the voltammetry and impedance results. There is a central hump in the positive sweep data near 0 V and rising capacitance starting at ≈ −0.5 V and 0.7 V. Notably, at the ends of the voltage range the capacitance does not decrease as in the impedance data but rather keeps increasing. As can be seen in Fig. 4, the current does not decay exactly to zero; however, at larger voltages ≈ ± 1 V, the constant offset became significantly larger, ≈50 nA. This may indicate that effects other than pure RC charging must be accounted for, and the data reliability in this region needs to be further investigated. PITT is, as far as we could find in literature, a new method for investigating the RTIL double layer capacitance. The data is noisier than in the other tests, and may benefit from larger electrode areas which would provide larger signals at the cost of RTIL consumption.

All three tests allow for calculation of differential capacitance as a function of potential. The trends are broadly similar, with a peak near open circuit potential and rising wings. As seen in the voltammetry results for the positive wing and in the impedance results for both limits, the wings may also peak and ultimately lead to decaying capacitance. Double layer theories that account for concentrated ions with finite size predict this decay in capacitance, as the double layer must become effectively thicker as the counterion density saturates and additional countercharge must build up in successive layers.

III.A. Comparison to theory

Referring back to Eq. 1, we can calculate an estimate for the capacitance from physical characteristics of [emim][BF_4]. A key question is, what is the appropriate length to use as the separation distance d? From classical theories, we may try an ion size a (Helmholtz) or the Debye length λ_D (Gouy-Chapman). However, these theories were developed for dilute electrolytes, and highly concentrated electrolytes including RTILs deviate far from their assumptions. Recent theoretical developments[11] and simulations[12,13] have shown that RTILs form multilayered structures at interfaces, with alternating layers of counterions and coions. Zhao used scaling analyses to conclude that a more appropriate length scale for RTILs with strong electrostatic correlations is $\sqrt{\lambda_D l_c}$, where l_c is the correlation length.[14] Using this, we get

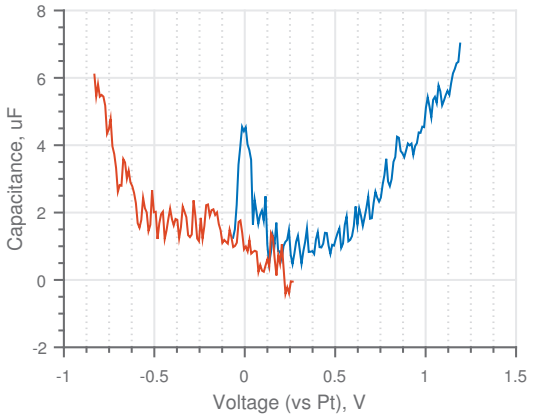

Figure 5. Capacitance values calculated from exponential fits to PITT data.

$$C = \frac{\epsilon_r \epsilon_0}{\sqrt{\lambda_D l_c}} A = \frac{\epsilon_r \epsilon_0}{\left(\frac{\epsilon_r \epsilon_0 k_B T}{2e^2 c_0}\right)^{1/4} l_c^{1/2}} A \tag{6}$$

We can estimate that $l_c \sim a$ and concentration $c_0 = \frac{\rho_m}{\bar{m}} N_A$ is found from the RTIL density ρ_m, molecular weight $\bar{m}$, and Avogadro's number N_A. There are many lists of RTIL physical parameters available,[15–17] and after plugging in numbers we get C =1.22 and 1.60 µF, for the two ion sizes and our electrode area.

The classical dilute Gouy Chapman theory predicts a capacitance curve that varies as $\sim \cosh \frac{zeV}{2k_B T}$, with a minimum at PZC. However, in order to get a better theoretical understanding of the RTIL capacitance curves, we must refer to theories that take steric effects of finite ion size and electrostatic correlations into account. Kornyshev developed a mean field theory with a lattice saturation parameter γ, where the dilute limit $\gamma = 0$ agrees with Gouy-Chapman and $\gamma \to 1$ approaches lattice saturation.[11] As γ increases, capacitance curves take on a "camel" shape with two humps straddling the local minimum (PZC), then a bell shape with maximum at PZC. Bazant, Storey, and Kornyshev proposed a continuum model with a correlation-length-dependent term in the free energy which captures the multilayered interface structure in overscreened and crowded regimes.[18] These models, while formulated for spherical ions of equal size, present a foundation from which to compare with data and parametrize the effects of asymmetrically-sized RTILs. Han, Huang, and Yan added an anion/cation volume ratio parameter ξ to a mean-field theory accounting for steric effects and observed, for certain conditions, two different sized humps qualitatively similar to our impedance results except the central hump.[19] Future efforts will include obtaining capacitance curves for RTILs with different ion size ratios and corroborating them with concentrated electrolyte theories.

III.B. Application to Electrospray Thrusters

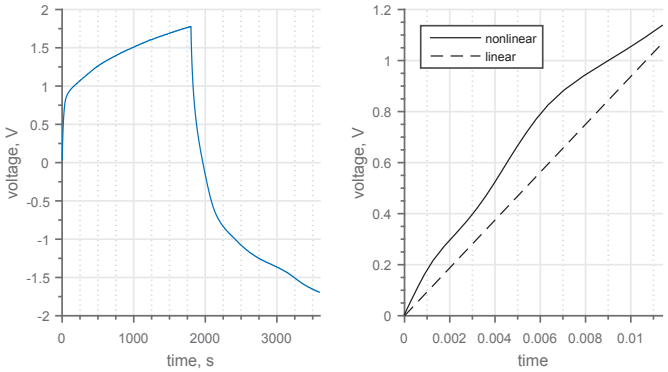

Figure 6. Left: Preliminary charging data for [emim][BF_4] at a porous RF electrode. Right: Comparison of nonlinear and linear capacitor charging.

The double layer drives the ion emission process and possible electrochemistry. Electrochemistry is the

result of the onset of Faradaic reactions, which break down the RTIL and may also damage the electrode surface. As ions are emitted during thruster operation, the opposite charge builds up at the interface in the double layer. Eventually the potential across this double layer breaches the electrochemical window and Faradaic reactions increase. Our current thrusters avoid critical electrochemical degradation with voltage alternation[7] and the utilization of a porous distal electrode.[8,20] However, in order to better guide future design we must understand how the double layer behaves. This work is the first step in understanding its structure and dynamics; as we refine our theoretical understanding in simple systems, we will continue our work by studying the double layers in more complex geometries. An expansion of this work will be to use the porous electrode materials in place of the platinum surfaces. Preliminary data, shown in Fig. 6, measured the voltage growth at a porous resorcinol-formaldehyde carbon aerogel electrode as a constant current of 150 µA was driven through [emim][BF_4]. This simulates real operating conditions of electrospray thrusters, and indicates that the increased surface area of $\approx 500\,\mathrm{m^2\,g^{-1}}$ results in charging times as long as 30 min as compared to the few seconds observed in the PITT test at a flat platinum surface. In such potential traces, deviation from an initial linear regime is often interpreted as onset of reactions. However, that assumes a linear capacitance as in Eq. 2; with nonlinear capacitance, the evolution of potential must account for the nonlinearity. We can use capacitance curves like those presented above and solve

$$I = \frac{dQ}{dt} = \frac{d}{dt}\left(CV\right) = \left(C + V\frac{dC}{dV}\right)\frac{dV}{dt} \tag{7}$$

for $V(t)$ using a constant input current I. Figure 6 shows how a capacitance which varies as in Fig. 3 may differ from a constant capacitance over some current-dependent time scale. Further decay of the potential growth will then indicate reaction onset and set a maximum period for voltage alternation in electrospray operation. Electrospray has already demonstrated feasibility as a space propulsion concept and scalability beyond any existing propulsion technology; further improvements in its underlying physics will continue to increase the capabilities of future spacecraft.

Acknowledgment

Financial support from NASA is gratefully acknowledged. We would like to express our gratitude to Prof. M.Z. Bazant (MIT) for useful discussions and use of laboratory equipment.

References

[1]Lozano, P. and Martínez-Sánchez, M., "Efficiency Estimation of EMI-BF_4 Ionic Liquid Electrospray Thrusters," *41st AIAA/ASME/SAE/ASEE Joint Propulsion Conference & Exhibit*, Tucson, AZ, 2005.

[2]Courtney, D. G., Li, H., Diaz Gomez Maqueo, P., Fedkiw, T. P., and Lozano, P. C., "On the Validation of Porous Nickel as Substrate Material for Electrospray Ion Propulsion," *46th AIAA/ASME/SAE/ASEE Joint Propulsion Conference & Exhibit*, Nashville, TN, 2010.

[3]Krejci, D., "Design and Characterization of a Scalable Ion Electrospray Propulsion System," *Joint Conference of 30th ISTS, 34th IEPC and 6th NSAT*, Hyogo-Kobe, Japan, 2015, In Press.

[4]García, L. F. V., Akinwande, A. I., and Martínez-Sánchez, M., "A Micro-fabricated Colloid Thruster Array," *38th AIAA/ASME/SAE/ASEE Joint Propulsion Conference & Exhibit*, Indianapolis, IN, 2002.

[5]Lozano, P., Glass, B., and Martínez-Sánchez, M., "Performance Characteristics of a Linear Ionic Liquid Electrospray Thruster," *29th International Electric Propulsion Conference*, Princeton, NJ, 2005.

[6]Jr., R. S. L., Lozano, P., and Martínez-Sánchez, M., "Fabrication and Characterization of Porous Metal Emitters for Electrospray Thrusters," *30th International Electric Propulsion Conference*, Florence, Italy, 2007.

[7]Lozano, P. and Martínez-Sánchez, M., "Ionic Liquid Ion Sources: Suppression of Electrochemical Reactions Using Voltage Alternation," *Journal of Colloid and Interface Science*, Vol. 280, No. 1, 2004, pp. 149–154.

[8]Brikner, N. and Lozano, P. C., "The Role of Upstream Distal Electrodes in Mitigating Electrochemical Degradation of Ionic Liquid Ion Sources," *Applied Physics Letters*, Vol. 101, No. 19, 2012.

[9]Lockett, V., Sedev, R., and Ralston, J., "Differential Capacitance of the Electrical Double Layer in Imidazolium-Based Ionic Liquids: Influence of Potential, Cation Size, and Temperature," *The Journal of Physical Chemistry C*, Vol. 112, No. 19, 2008, pp. 7486–7495.

[10]Lockett, V., Horne, M., Sedev, R., Rodopoulos, T., and Ralston, J., "Differential Capacitance of the Double Layer at the Electrode/Ionic Liquids Interface," *Physical Chemistry Chemical Physics*, Vol. 12, No. 39, 2010, pp. 12499–12512.

[11]Kornyshev, A. A., "Double-Layer in Ionic Liquids: Paradigm Change?" *The Journal of Physical Chemistry B*, Vol. 111, No. 20, 2007, pp. 5545–5557.

[12]Fedorov, M., Georgi, N., and Kornyshev, A., "Double layer in ionic liquids: The nature of the camel shape of capacitance," *Electrochemistry Communications*, Vol. 12, No. 2, 2010, pp. 296–299.

[13]Merlet, C., Rotenberg, B., Madden, P. A., and Salanne, M., "Computer simulations of ionic liquids at electrochemical interfaces," *Physical Chemistry Chemical Physics*, Vol. 15, No. 38, 2013, pp. 15781–15792.

[14]Zhao, H., "Diffuse-charge Dynamics of Ionic Liquids in Electrochemical Systems," *Physical Review E*, Vol. 84, No. 5, 2011.

[15]Liu, S., Liu, W., Liu, Y., Lin, J.-H., Zhou, X., Janik, M. J., Colby, R. H., and Zhang, Q., "Influence of Imidazolium-based Ionic Liquids on the Performance of Ionic Polymer Conductor Network Composite Actuators," *Polymer International*, Vol. 59, No. 3, 2010, pp. 321–328.

[16]Weingärtner, H., "The Static Dielectric Constant of Ionic Liquids," *Zeitschrift für Physikalische Chemie*, Vol. 220, No. 10, 2006, pp. 1395–1405.

[17]Zhang, S., Sun, N., He, X., Lu, X., and Zhang, X., "Physical Properties of Ionic Liquids: Database and Evaluation," *Journal of Physical and Chemical Reference Data*, Vol. 35, No. 4, 2006, pp. 1475–1517.

[18]Bazant, M. Z., Storey, B. D., and Kornyshev, A. A., "Double Layer in Ionic Liquids: Overscreening Versus Crowding," *Physical Review Letters*, Vol. 106, No. 4, 2011.

[19]Han, Y., Huang, S., and Yan, T., "A Mean-field Theory on the Differential Capacitance of Asymmetric Ionic Liquid Electrolytes," *Journal of Physics: Condensed Matter*, Vol. 26, No. 28, 2014.

[20]Arestie, S. M., *Porous Material and Process Development for Electrospray Propulsion Applications*, Master's thesis, Massachusetts Institute of Technology. Department of Aeronautics and Astronautics, Cambridge, MA, 2014.